Available online at www.sciencedirect.com

ScienceDirect

Ceramics International 40 (2014) 4553–4557

CERAMICS INTERNATIONAL

www.elsevier.com/locate/ceramint

Preparation of controlled-shape ZnS microcrystals and photocatalytic property

Shujuan Zhang*

College of Science, Tianjin University of Science & Technology, Tianjin, 300457, PR China

Received 30 June 2013; received in revised form 30 August 2013; accepted 30 August 2013
Available online 7 September 2013

Abstract

ZnS microcrystals with various shapes, including polyhedron, fan-shaped sheet, hexagonal rectangle and missing angle rectangle, were successfully prepared using a simple hydrothermal method by changing the experimental conditions. The as-obtained ZnS samples were characterized by X-ray diffraction, scanning electron microscopy and energy-dispersive X-ray spectroscopy. The photocatalytic activities of the ZnS microcrystals with different morphologies were investigated by degradation testing of methylene blue aqueous solution. The highest photodegradation rate of methylene blue over the polyhedron-shaped ZnS reached up to almost 100%. The photodegradation efficiencies under various conditions, including amount of catalyst, pH of aqueous solution and initial concentration of methylene blue, were studied in the presence of polyhedron-shaped ZnS. The polyhedron-shaped ZnS microcrystal can thus be utilized as a promising photocatalyst for photodegrading dyes in wastewater treatment.

Keywords: ZnS; Various shape; Photodegradation

1. Introduction

Over the past few decades, semiconductor photocatalysts are becoming increasingly attractive because of the potential in solving environmental pollution issues [1–5]. However, the application is limited because TiO_2 can only be excited by UV light, although TiO_2 is generally recognized as the most photoactive catalyst among semiconductors [6–8]. New photocatalytic materials, such as sulfides [9], halides [10], composite oxides [11] and organic polymers [12], have been developed. Metal sulfides have become spotlighted photocatalysts owing to narrow band gap, good light absorption properties and excellent photocatalytic performance. Zhou et al. synthesized SnO_2-decorated SnS_2 nanosheets with enhanced visible light photocatalytic activity by a one-pot solvothermal process using $SnCl_4 \cdot 5H_2O$ and CH_4N_2S as precursors [13]. Cheng et al. synthesized Bi_2S_3/BiOCl hybrid architectures with tunable band gaps by a controlled anion exchange approach and they displayed highly efficient visible light photoactivities [14].

In these metal sulfides, ZnS, which is an important semiconductor with the band gap energy of 3.6 eV, has been widely applied in catalysts, electronic modulators, field-effect transistors, and light-emitting materials [15]. Hu et al. first prepared photocatalytically active ZnS nanoparticles sized 3–5 nm in 2005 [16]. Chen et al. synthesized 3D ZnS microspheres composed of 20–30 nm interwoven nanosheets, exhibiting higher photocatalytic activity [17]. Liu et al. prepared unusually extended and oriented wurtzite ZnS nanorods/nanowires by a one-pot wet chemical method. The layered ZnS nanorods/nanowires had extraordinary photocatalytic ability for the photodegradation of non-biodegradable brilliant red X-3B azo dye under UV-light irradiation [18]. ZnS can effectively photodegrade organic dyes, and high energy conversion efficiencies as well as light-harvesting abilities can be obtained by constructing photocatalysts with various architectures [9]. Thus, ZnS with various micro and nanostructures are of superb photocatalytic efficiencies [15]. In this study, ZnS with various structures, including polyhedron, fan-shaped sheet, hexagonal

*Corresponding author. Tel./fax: +86 22 83955458.
E-mail address: songlmnk@sohu.com

0272-8842/$ - see front matter
http://dx.doi.org/10.1016/j.ceramint.2013.08.131

rectangle and missing-angle rectangle, were prepared successfully. The photodegradation activity of the polyhedron-shaped microcrystal was best among different samples under light radiation, confirming that ZnS with diverse structures exhibited various photocatalytic properties. Besides, the photocatalytic activities of polyhedron-shaped ZnS were studied in detail under different conditions.

2. Experimental

2.1. Synthesis of samples

In a typical process, 1.83 g $Zn(NO_3)_2 \cdot 6H_2O$ and 1.49 g $Na_2S \cdot 9H_2O$ were dissolved in 30 mL of deionized water under stirring. The above solution was transferred into a 50 mL stainless steel autoclave. A piece of Cd slice was placed in the autoclave to get samples. The autoclave was kept at 180 °C for 12 h in an oven. All other experiments were performed using the same procedure. When the autoclave was cooled down to the room temperature, the precipitate was collected and washed with deionized water and finally dried in the oven at 120 °C for 3 h. Fan-shaped ZnS slice was obtained instead if deionized water was replaced with ethylenediamine ($C_2H_8N_2$) while other conditions were maintained unchanged. Hexagonal rectangle ZnS was prepared if sodium dodecyl sulfate (SDS, $C_{12}H_{25}O_4SNa$) was added to the reaction and deionized water was still used as the solvent. Missing angle rectangle ZnS was prepared if SDS was substituted for polyethyleneglycol [PEG, $(OHCH_2CH_2HO)_n$].

2.2. Characterization of samples

X-ray diffraction patterns were recorded using a Rigaku D/max 2500 analytical diffractometer with the scanning angle from 10° to 80°. Morphologies of the samples were examined using a Hitachi S-4800 field emission scanning electron microscope with an energy dispersive mode. Accelerating voltage of field emission scanning electron microscope was set at 10 kV. UV–visible absorption spectra were recorded using a Shimadzu UV-2550PC spectrophotometer.

2.3. Activity measurement

All the photocatalytic experiments were carried out in a 250 mL home-made reactor. Methylene blue (MB) was photodegraded at room temperature by purging air. In a typical experiment, 100 mL of 10 mg/L MB aqueous solution containing 0.3 g photocatalyst was used. The above mixture was stirred in dark for 30 min to reach adsorption equilibrium on the photocatalyst surface prior to photocatalysis. A 400 W high pressure mercury lamp (365 nm) was used as the irradiation source. At regular intervals, 5 ml solution was withdrawn and centrifuged to remove the catalyst. Finally, the absorbance of the solution was measured at 665 nm to calculate the photocatalytic activity.

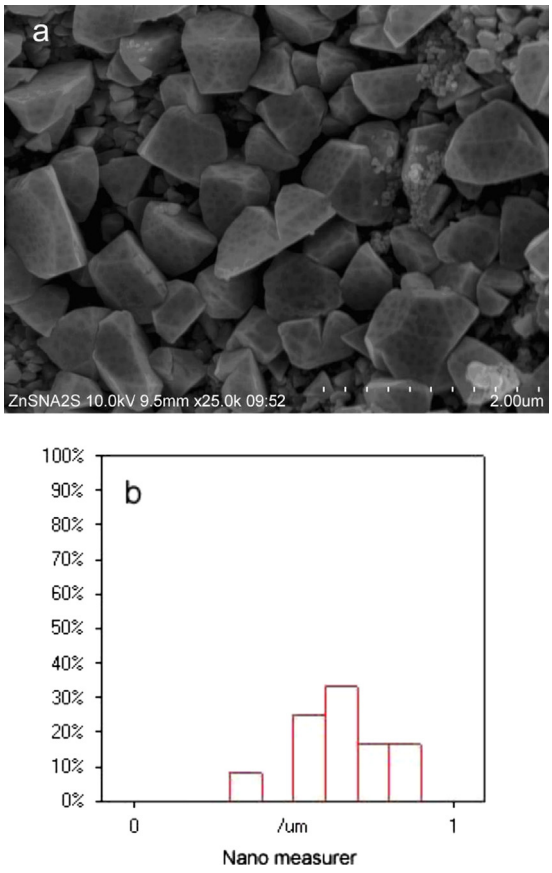

Fig. 1. (a) SEM images and (b) particle mean size distribution curve of the polyhedron-shaped ZnS microstructures.

3. Results and discussion

3.1. Characterization of photocatalysts

Morphology of the as-prepared sample in a typical process (1.83 g $Zn(NO_3)_2 \cdot 6H_2O$, 1.49 g $Na_2S \cdot 9H_2O$, 30 mL of deionized water) was characterized by field emission scanning electron microscope (FESEM) as shown in Fig. 1a in which a large number of polyhedron-shaped ZnS microstructures can be observed. Typical three-dimensional (3D) polyhedron structures with the average diameter of 0.64 μm are densely packed. These polyhedrons can be regarded as cubes from which many angles have been cut away. Many dotted spots can be discerned on the surface of the polyhedrons. The average particle size distribution curve of the polyhedrons is shown in Fig. 1b, revealing that the maximum and minimum particle sizes are 0.83 μm and 0.39 μm, respectively.

Phase composition and structure of the as-synthesized polyhedron-shaped sample were investigated by X-ray diffraction (XRD) (Fig. 2A). The strong peaks at 28.78°, 47.58°, and 56.7° can be assigned to the (108), (110), and (028) planes of hexagonal phase with the lattice constants of $a=b=3.823$ Å, $c=74.976$ Å (JCPDS no. 89-2349), without other impurities being detected. Energy dispersive mode (EDS) (Fig. 2B) shows that the polyhedron-shaped ZnS crystal consists of Zn and S elements. Traces of other elements, including C, O, Al,

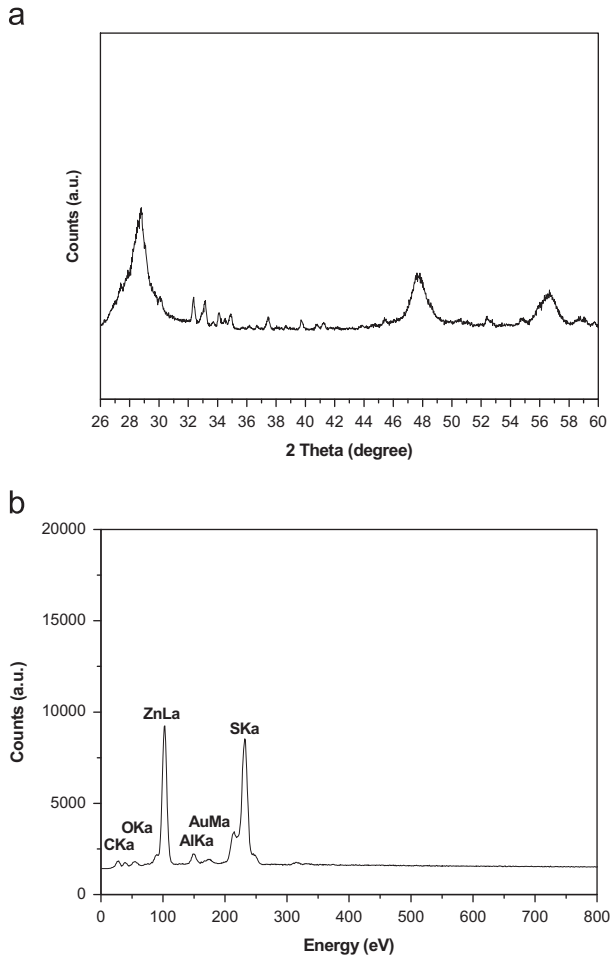

Fig. 2. X-ray diffraction and EDS patterns of the polyhedron-shaped ZnS microstructures.

and Au, can be assigned to contaminated carbon, the air-oxidized Zn, the Al supporter, and the sputtered Au film, respectively. The ratio of Zn to S is approximately 32.34: 29.74, nearly equaling the stoichiometry (1:1).

In order to understand various morphologies of ZnS, ZnS samples were synthesized under different experimental conditions. If H_2O was substituted with ethylenediamine ($C_2H_8N_2$) in the reaction system while other conditions were maintained unchanged, fan-shaped ZnS slice microstructures (Fig. 3a) were obtained, some of which closely stacked layeredly. The magnified image of typical ZnS microslices (Fig. 3b) shows that a fan-shaped microstructure radiates from the center. These fans have the radii of about 10 μm and the lengths ranging between 20 and 40 μm. A large number of hexagonal rectangles were obtained upon the addition of 0.18 g sodium dodecyl sulfate (SDS, $C_{12}H_{25}O_4SNa$) (Fig. 3c). Hexagonal rectangles indicate that the as-obtained ZnS is a hexagonal phase. Fig. 3d shows the high-magnification SEM image of typical hexagonal rectangles with smooth surfaces, from which four angles seem missing. The widths of the nanoplatelets are typically 0.1–1 μm, their lengths range between 0.5 and 2 μm, and their thickness is approximately 0.1 μm. If SDS was replaced with polyethyleneglycol [PEG, $(OHCH_2CH_2HO)_n$], the missing angle rectangles can be retrieved (Fig. 3e). However, the rectangles are obviously different from those without rectangle angles and four vertices in Fig. 3c. Therefore, no hexagonal rectangles formed.

3.2. Photocatalytic activity of photocatalysts

The photodegradation rates of ZnS microcrystals with different morphologies (polyhedron, fan-shaped sheet, hexagonal rectangle, and missing angle rectangle) against MB were evaluated at the intervals of 10 min within 60 min. A mixture of ZnS powders and MB solution was stirred in dark for 30 min to reach adsorption equilibrium on ZnS surface before light radiation. The photodegradation curve of fan-shaped sheet ZnS is not shown in Fig. 4 because the adsorption rate of MB exceeded 91%. With elapsed light irradiation time, the photodegradation rates of polyhedron and missing angle rectangle ZnS increased gradually, whereas that of hexagonal rectangle ZnS did not evidently change. Besides, the photodegradation rate of polyhedron ZnS reached up to about 93% after 60 min, whereas that of missing angle rectangle ZnS was only about 61%. It is well known that various morphologies of ZnS microcrystals that expose different crystal faces are of significantly different activities, which has also been confirmed herein. In this study, polyhedron ZnS is of the highest activity in all the ZnS samples.

As is known to all, photocatalytic activity is also affected by the amount of photocatalyst. Therefore, the effects of 2.25–3.75 g/L polyhedron ZnS were studied. Fig. 5 shows that the photodegradation rates of MB increase with increasing amount of the polyhedron ZnS after 60 min, which are 82%, 91%, and 93%, respectively. In addition, the photodegradation rate increased from 83% to 93% when the photocatalyst concentration rose from 2.25 to 3 g/L. However, the photodegradation rate maintained almost constant when the photocatalyst concentration increased from 3 to 3.75 g/L. More active sites of the photocatalyst were exposed on the surface by adding excess photocatalyst in the reaction system. Therefore, more •OH radicals formed, allowing the higher oxidative ability of the photocatalyst. The amount of •OH radicals in the reaction system ceased increasing by maintaining other conditions unchanged when the photocatalyst amount exceeded a certain threshold. Therefore, the degradation rate of MB changed slowly.

MB photodegradation by polyhedron ZnS was studied from pH 7–13. Taking into consideration that MB molecules decomposed and ZnS particles dissolved easily under acidic conditions, we only investigated the activity of ZnS in the MB solution at pH higher than 7. Fig. 6 shows that the adsorption rate of MB changes distinctly with increasing pH. The adsorption rates are 10%, 19%, 42%, and 60% respectively at pH from 7 to 13, denoting that alkaline environment facilitated the adsorption of MB molecules on the ZnS surface. Given that catalytic reaction is a surface process, MB molecules are first adsorbed on the surface of ZnS particles and then oxidized by •OH radicals. The photodegradation rates of MB are 93%, 39%, 92%, and 93% respectively with

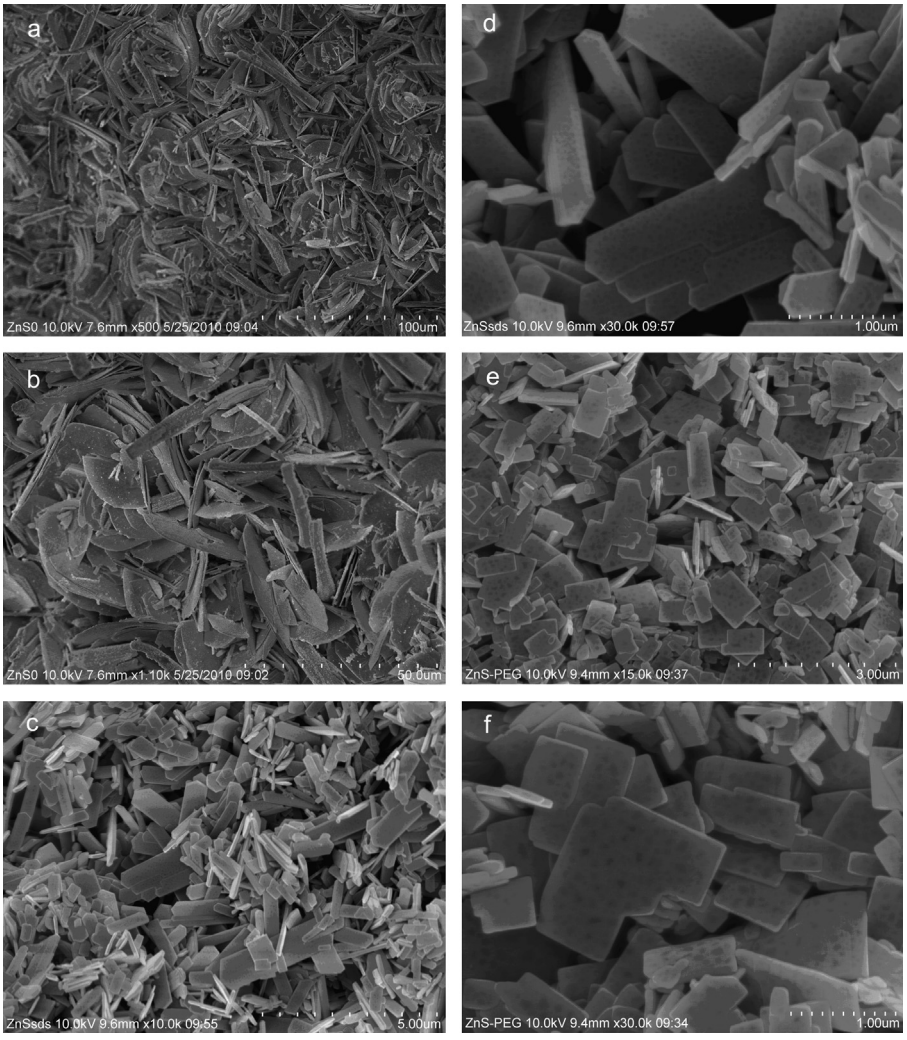

Fig. 3. SEM images of the ZnS microstructures. (a) and (b) fan-shaped microslices, (c) and (d), hexagonal rectangles (e) and (f) missing angle rectangles.

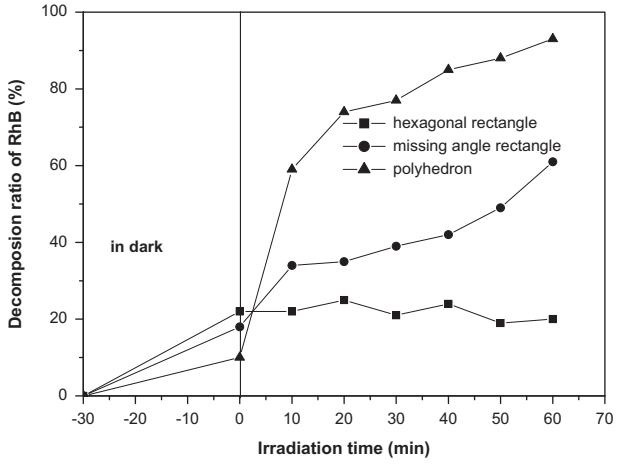

Fig. 4. The dependence of photocatalytic activity on the ZnS samples with various shapes.

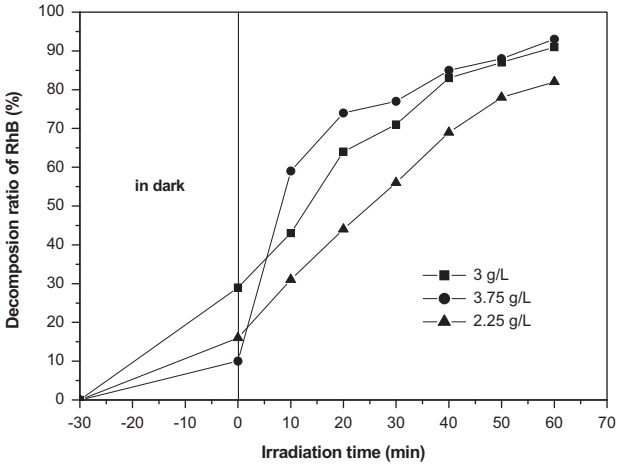

Fig. 5. The dependence of photocatalytic activity on the ZnS amount.

increasing pH (from 7 to 13). The enhanced activity is attributed to the increased adsorption rate of MB on ZnS surface. Moreover, the photodegradation rate of MB was lowest at pH 8 because the adsorption rate was merely 19%.

Initial MB concentrations ranging from 5 to 20 mg/L were used to study the photocatalytic activity of polyhedron ZnS. As shown in Fig. 7, the photodegradation rate of MB increases with elevating MB concentration. The photodegradation efficiencies

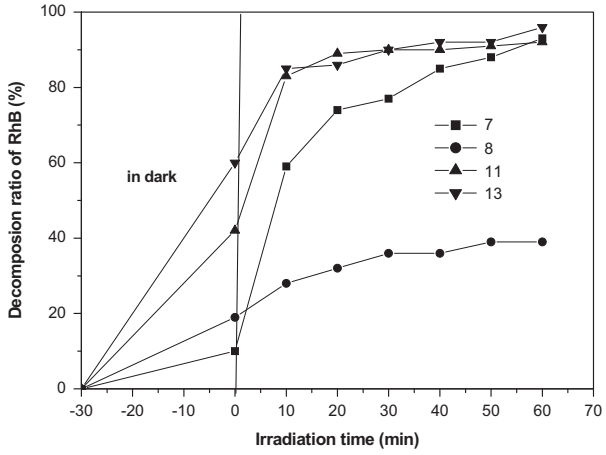

Fig. 6. The dependence of photocatalytic activity on the pH values of MB solution.

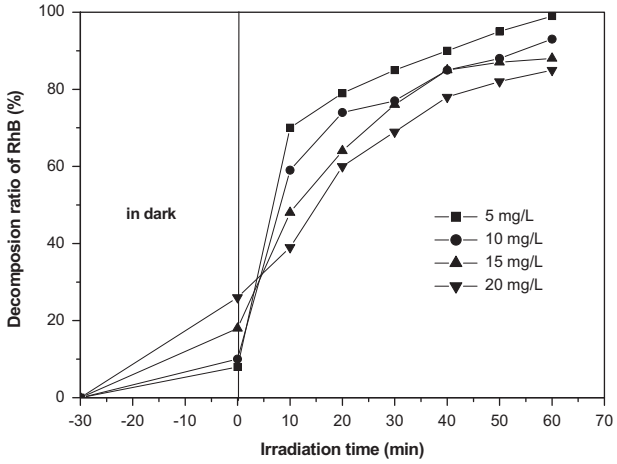

Fig. 7. The dependence of photocatalytic activity on the original concentration of MB solution.

are 99%, 93%, 88%, and 85% respectively in the presence of 5–20 mg/L MB. Besides, a high initial MB concentration is conducive to the adsorption of MB molecules on the surface of ZnS particles, and a higher adsorption amount will boost the photocatalytic activity. Moreover, a high initial MB concentration can enhance the opportunities of MB molecules encountering •OH radicals produced by light irradiation, so that more MB molecules can be oxidized by •OH radicals.

4. Conclusions

In summary, ZnS with various shapes were synthesized successfully. Polyhedron ZnS shows the best photodegradation activity against MB under light radiation in all the ZnS samples, which can be ascribed to the different exposed crystal faces and the active sites of ZnS microcrystals with diverse shapes, demonstrating that the photocatalytic abilities of different crystal faces against the same crystal significantly differ.

References

[1] R. Asahi, T. Morikawa, T. Ohwaki, K. Aoki, Y. Taga, Visible-light photocatalysis in nitrogen-goped titanium oxides, Science 293 (2001) 269–271.
[2] S.U.M. Khan, M.A. Shahry, W.B. Ingler, Efficient photochemical water splitting by a chemically modified n-TiO_2, Science 297 (2002) 2243–2245.
[3] I. Justicia, P. Ordejon, G. Canto, Designed self-doped titanium oxide thin films for efficient visible-Light photocatalysis, Advanced Materials 14 (2002) 1399–1402.
[4] U.G. Akpan, B.H. Hameed, Parameters affecting the photocatalytic degradation of dyes using TiO_2-based photocatalysts: a review, Journal of Hazardous Materials 170 (2009) 520–529.
[5] P. Li, Z. Wei, T. Wu, Q. Peng, Y.D. Li, Au–ZnO hybrid nanopyramids and their photocatalytic properties, Journal of the American Chemical Society 133 (2011) 5660–5663.
[6] T.R. Gordon, M. Cargnello, T. Paik, F. Mangolini, R.T. Weber, P. Fornasiero, C.B. Murray, Nonaqueous synthesis of TiO_2 nanocrystals using TiF_4 to engineer morphology, oxygen vacancy concentration, and photocatalytic activity, Journal of the American Chemical Society 15 (2012) 6751–6761.
[7] M. Bellardita, M. Addamo, A.D. Paola, G. Marcì, L. Palmisano, L. Cassar, M. Borsa, Photocatalytic activity of TiO_2/SiO_2 systems, Journal of Hazardous Materials 174 (2010) 707–713.
[8] J.B. Zhong, Y. Lu, W.D. Jiang, Q.M. Meng, X.Y. He, J.Z. Li, Y.Q. Chen, Characterization and photocatalytic property of Pd/TiO_2 with the oxidation of gaseous benzene, Journal of Hazardous Materials 168 (2009) 1632–1635.
[9] Q.R. Zhao, Y. Xie, Z.G. Zhang, X. Bai, Size-selective synthesis of zinc sulfide hierarchical structures and their photocatalytic activity, Crystal Growth & Design 7 (2007) 153–158.
[10] P. Wang, B.B. Huang, X.Y. Qin, H. Jin, Y. Dai, Z.Y. Wang, J.Y. Wei, J. Zhan, S.Y. Wang, J.P. Wang, M.H. Whangbo, Highly efficient visible-light plasmonic photocatalyst Ag@AgBr, Chemistry. A European Journal 15 (2009) 1821–1824.
[11] Z.G. Yi, J.H. Ye, N. Kikugawa, T. Kako, S.X. Ouyang, H.S. Williams, H. Yang, J.Y. Cao, W.J. Luo, Z.S. Li, Y. Liu, R.L. Withers, An orthophosphate semiconductor with photooxidation properties under visible-light irradiation, Nature Materials 9 (2010) 559–564.
[12] J.H. Sun, J.S. Zhang, M.W. Zhang, M. Antonietti, X.Z. Fu, X.C. Wang, Bioinspired hollow semiconductor nanospheres as photosynthetic nanoparticles, Nature Communications 16 (2012) 1–7.
[13] X.L. Zhou, T.F. Zhou, J.C. Hu, J.L. Li, Controlled strategy to synthesize SnO_2 decorated SnS_2 nanosheets with enhanced visible light photocatalytic activity, CrystEngComm 14 (2012) 5627–5633.
[14] H.F. Cheng, B.B. Huang, X.Y. Qin, X.Y. Zhang, Y. Dai, A controlled anion exchange strategy to synthesize Bi_2S_3 nanocrystals/BiOCl hybrid architectures with efficient visible light photoactivity, Chemical Communications 48 (2012) 97–99.
[15] Y. Zhang, Y.D. Li, Synthesis and characterization of monodisperse doped ZnS nanospheres with enhanced thermal stability, Journal of Physical Chemistry B 108 (2004) 17805–17811.
[16] J.S. Hu, L.L. Ren, Y.G. Guo, H.P. Liang, A.M. Cao, L.J. Wan, C.L. Bai, Mass production and high photocatalytic activity of ZnS nanoporous nanoparticles, Angewandte Chemie International Edition 44 (2005) 1269–1273.
[17] D.G. Chen, F. Huang, G.Q. Ren, D.S. Li, M. Zheng, Y.J. Wang, Z. Lin, ZnS nano-architectures: photocatalysis, deactivation and regeneration, Nanoscale 2 (2010) 2062–2064.
[18] Y. Liu, J.C. Hu, T.F. Zhou, R.C. Che, J.L. Lia, Self-assembly of layered wurtzite ZnS nanorods/nanowires as highly efficient photocatalysts, Journal of Materials Chemistry 21 (2011) 16621–16627.